AIP Applied Physics Letters

Lithium manganese oxide as an effective buffer layer between organic and metal layers in organic light-emitting devices

Tswen-Hsin Liu

Citation: Applied Physics Letters **89**, 102101 (2006); doi: 10.1063/1.2339028
View online: http://dx.doi.org/10.1063/1.2339028
View Table of Contents: http://scitation.aip.org/content/aip/journal/apl/89/10?ver=pdfcov
Published by the AIP Publishing

Lithium manganese oxide as an effective buffer layer between organic and metal layers in organic light-emitting devices

Tswen-Hsin Liu[a)]

Department of Photonics, National Chiao Tung University, Hsinchu 300, Taiwan, Republic of China; Institute of Electro-Optical Engineering, National Chiao Tung University, Hsinchu 300, Taiwan, Republic of China; and AU Optronics Corporation, Hsinchu 300, Taiwan, Republic of China

(Received 6 March 2006; accepted 7 July 2006; published online 5 September 2006)

Tris(8-hydroxyquinolinato)aluminum (Alq_3)-based organic light-emitting devices using a thermally deposited lithium manganese oxide layer between aluminum (Al) cathode and Alq_3 have been fabricated. The highest luminance efficiency obtained with a 1-nm-thick $LiMn_xO_y$ layer is very similar to that of the device with 1-nm-thick LiF. However, the device with an 18 nm $LiMn_xO_y$ layer obtained a longer operational stability although the luminance efficiency is lower. The improvements are attributed to lithium extractions of the lithium manganese oxide layer and the interfacial properties between Alq_3 and Al are discussed. © *2006 American Institute of Physics*. [DOI: 10.1063/1.2339028]

Organic light-emitting devices (OLEDs) are charge injection devices consist of organic thin layers that are essentially insulating materials. It is, therefore, important to reduce barrier heights for the carrier injection at the organic/electrode interfaces to realize low driving voltages and to balance the hole and electron injections to achieve high quantum efficiency. For improving electron injection, several cathode materials have been developed. Mg:Ag was the first alloy cathode and was introduced by Tang and Van Slyke in 1987.[1] Later, lithium-based cathodes such as Al:Li alloy[2] and a double-layer cathode of Li/Al (Ref. 3) were developed to reduce the driving voltage. Double-layer cathodes using a thin cathode interface layer, such as Li_2O/Al (Ref. 4) and LiF/Al,[5] were also developed and are now widely used. Recently, Kido and Matsumoto demonstrated an effective electron-injection system by using a Li-doped organic layer with a molecular ratio of Li/Alq_3 at unity.[6] In OLEDs with a configuration of indium tin oxide (ITO)/N,N'-bis(1-naphthyl)-N,N'-diphenyl-1,1′-biphenyl-4,4′ diamine (NPB)/tris(8-hydroxyquinolinato)aluminum (Alq_3)/Li-doped Alq_3/Al, the current density increases dramatically with increasing the thickness of the doped Alq_3 layer.

Lithium manganese oxide, $LiMn_2O_4$, is one of the most prominent materials used as cathode for rechargeable lithium batteries.[7] The lattice electronic conductivity of amorphous $LiMn_2O_4$ can reach values of 2×10^{-5}–5×10^{-5} S cm^{-1},[7,8] which is well described by a hopping conduction model with an activation energy of about 0.16 eV, declaring that the electron exchange between Mn^{3+} and Mn^{4+} ions should be responsible for the conductive property.[7,9] The melting point of commercial $LiMn_2O_4$ powder is around 400 °C; hence, it is appropriate to form film by thermal evaporation, which is commonly used in OLEDs. In this letter, we report the possibility of employing thermally deposited $LiMn_xO_y$ as an electron-injection layer for efficient and stable OLEDs.

The devices used in this study have a multilayer structure of ITO/copper phthalocyanine (CuPc)/NPB/Alq_3, where CuPc is the hole-injection layer, NPB is the hole-transport layer, and Alq_3 is the emission as well as electron-transport layer. All organic layers were prepared by conventional vapor deposition at ambient temperature.[10] The thicknesses were 15, 60, and 75 nm, for CuPc, NPB, and Alq_3, respectively. A layer of $LiMn_xO_y$ or LiF was subsequently deposited from a tungsten boat. Without breaking vacuum, the top electrode was prepared by sequential deposition of a thick Al overlayer using resistive heating. The electrochemical grade (99.99%) $LiMn_2O_4$ powder in this study was purchased from Aldrich and used without further purification. The thickness of each layer was monitored by a calibrated quartz thickness monitor. In particular, the tooling factor of $LiMn_xO_y$ was calculated according to the thickness measured by scanning electron microscope.

The current density and luminance as a function of operating voltage for OLEDs that contain the $LiMn_xO_y$ thicknesses (0, 1, 6, 18, 30, and 42 nm) or 1 nm LiF are shown in Figs. 1(a) and 1(b), respectively. It can be seen that by inserting the $LiMn_xO_y$ layers between Alq_3 and Al both the current-voltage (*I-V*) and luminance-voltage (*L-V*) curves are shifted towards a lower voltage. However, there are no significant differences in *I-V* and *L-V* characteristics in devices with different $LiMn_xO_y$ layer thicknesses. As the anode contact for hole injection in all these devices was the same, this also indicates that the presence of a $LiMn_xO_y$ layer be-

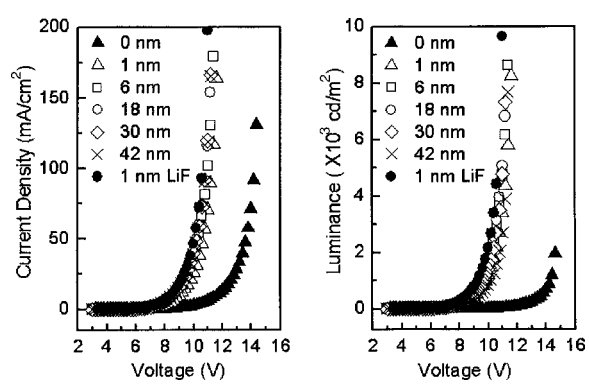

FIG. 1. *I-V* and *L-V* characteristics of a series of device with different $LiMn_xO_y$ thicknesses and 1 nm LiF.

[a)]Author to whom correspondence should be addressed; electronic mail: peteliu@auo.com

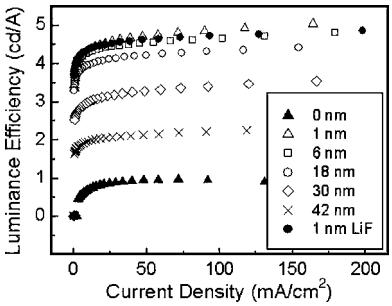

FIG. 2. Absorption spectrum of a deposited $LiMn_xO_y$ film taken at room temperature in the wavelength range of 250–850 nm. Inset: Normalized electroluminescent spectra of a series of device with different thicknesses of $LiMn_xO_y$ at 20 mA/cm^2.

tween Alq_3 and Al in Alq_3-based OLEDs greatly improves the electron injection over a wide range of thicknesses.

Figure 2 exhibits the plot of luminance efficiency along with the applied current density. It is clear that the device with 1-nm-thick $LiMn_xO_y$ displayed the highest luminance efficiency (~5 cd/A) among the devices, which is approximately five times higher than the $LiMn_xO_y$-free device. Gap states, which act as quenching centers, resulting from chemical bonding between Al and Alq_3 at the Al/Alq_3 interface, have been suspected to be one of the causes behind the poor performance seen in OLEDs based on Al cathode.[11–13] The results have indicated that a $LiMn_xO_y$ thickness of only 1 nm is sufficient to remove these states completely by avoiding a direct contact between Al and Alq_3.[14] However, a further increase in the $LiMn_xO_y$ layer thickness may result in a gradual decrease in efficiency. It is understood that the addition of a $LiMn_xO_y$ layer between Alq_3 and Al will alter the internal electric field distribution leading to a change in both the hole and electron injections. The attenuation in luminance efficiency of the devices due to the presence of $LiMn_xO_y$ layers between Alq_3 and Al might results from a less balanced charge injection. On the other hand, Fig. 3 shows the optical absorption spectrum of a deposited $LiMn_xO_y$ film in the wavelength range of 250–800 nm. A sizable absorption was observed at visible light regime. The inset of Fig. 3 also shows the electroluminescent spectra of the devices driven at 20 mA/cm^2. Obviously, the optical length between the reflective cathode and the half mirror ITO for these devices has been changed by inserting different thicknesses of $LiMn_xO_y$ films. The spectrum shifts to the longer-wavelength regime indicate that electroluminescence

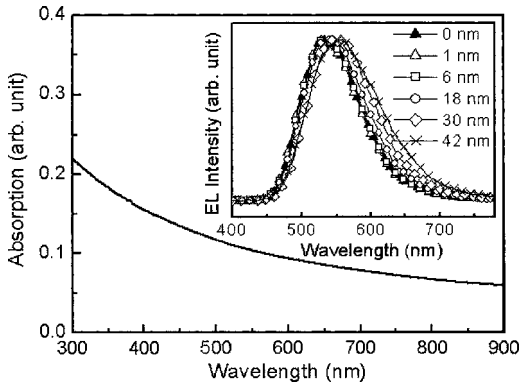

FIG. 3. Luminance efficiency vs current density curves of devices made with different $LiMn_xO_y$ thicknesses and 1 nm LiF.

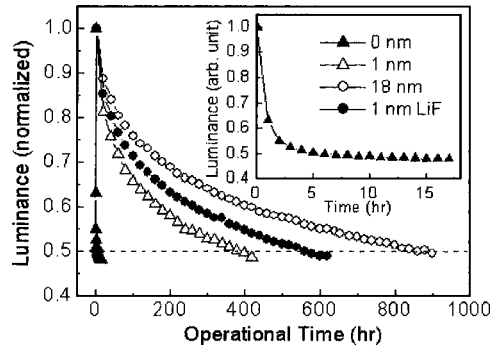

FIG. 4. Normalized luminance as a function of operational time for the devices with 0, 1, and 18 nm $LiMn_xO_y$ and 1 nm LiF. Inset: The device without the lithium manganese oxide or LiF layer shows distinctly separate time scales in the luminance decay.

was enhanced at red wavelengths and was suppressed at green wavelengths. Therefore, the deterioration of luminance in the thicker $LiMn_xO_y$ domain might also result from the destructive interference of green light in the half-cavity OLEDs incorporated with the light absorption property of $LiMn_xO_y$.

At present, the physical origin of the improved electron-injection characteristics is not certain. Previous studies on the LiF/Al double-layer cathode have revealed that the thermodynamically allowed reaction, expressed as $3LiF+Al+3Alq_3 \rightarrow AlF_3+3Li^+Alq_3^-$,[15–17] can induce electron injection due to the formation of a thin *n*-doped Alq_3 layer as in the cases of using Li-doped Alq_3 as the electron-injection layer or using Li as the low-work-function cathode.[6,18] Similarly, the chemical reactions [e.g., $3LiMn_xO_y+Al+3Alq_3 \rightarrow Al(Mn_xO_y)_3+3Li^+Alq_3^-$] at the interface of Al, $LiMn_xO_y$, and Alq_3 to generate $3Li^+Alq_3^-$ are also possible. However, the results suggest that the high injected current was also achieved at larger $LiMn_xO_y$ thicknesses. It is unlikely that Al, $LiMn_xO_y$, and Alq_3 will contact each other to undergo reactions considering the coverage of $LiMn_xO_y$ at the thicknesses of 18, 30, and 42 nm. Since electrochemical extraction of Li ions in $LiMn_2O_4$ cathode occurs at 4 V in rechargeable lithium batteries,[7] therefore, it is more likely due to the lithium extraction of $LiMn_xO_y$ at $LiMn_xO_y$/Al interface, and forms a Li–Al alloy at the interface. Nevertheless, when a bilayer cathode of $LiMn_xO_y$ (18 nm)/Al (200 nm) is acting as an electron-injection contact on an Alq_3 layer, the Li ions extracted at $Alq_3/LiMn_xO_y$ interface can form a thin *n*-doped Alq_3 layer and is advantageous for reducing the electron-injection barrier to Alq_3 layer.

Figure 4 shows the operational stability driven at 40 mA/cm^2 for devices that contain typical $LiMn_xO_y$ thicknesses (0, 1, and 18 nm) as well as device with 1 nm LiF. One noteworthy feature in the inset of Fig. 4 is the occurrence of two distinctly separate time scales in the luminance decay when there is no buffer layer between Al and Alq_3, with an early rapid decay to 50% of the initial luminance at the initial 5 h. This instability may be attributed to a number of factors, including the formation of deep carrier traps in the bulk, interface degradation, and mismatch between the Fermi level of the Al layer and the lowest unoccupied molecular orbital edge of the Alq_3 layer.[19] However, by adding a $LiMn_xO_y$ or LiF buffer layer of a suitable thickness between Alq_3 layer and Al cathode, reliability can be significantly improved. As mentioned in Fig. 2, the highest luminance

efficiency is obtained with a $LiMn_xO_y$ thickness of 1 nm, which is very similar to that of the device with 1-nm-thick LiF. But the device incorporating a 1-nm-thick $LiMn_xO_y$ shows a lower operational stability than the conventionally used LiF device. The longer operational stability can be obtained by the device with 18-nm-thick $LiMn_xO_y$, which shows a somewhat lower efficiency than the one using 1 -nm-thick LiF. The work of Zhan *et al.* shows that a sodium stearate buffer layer can improve current injection and device thermal stability of the OLEDs, as a result of the decrease of the interfacial roughness at Alq_3/Al.[20] Since the electron injection is nearly independent of the $LiMn_xO_y$ thickness over the range of 1–42 nm in Fig. 1, we suspect that the difference in the interfacial stability between Alq_3, $LiMn_xO_y$, and Al owing to morphology change of the thicker $LiMn_xO_y$ may very well play a role to enhance the durability. In our atomic force microscopy (AFM) studies, an Alq_3 film with a thickness of 75 nm was evaporated on an ITO-coated glass substrate, and then 1-nm-thick or 18-mm-thick $LiMn_xO_y$ was deposited on the top. AFM images of the 1-mm-thick $LiMn_xO_y/Alq_3$ film showed flat surfaces with a mean roughness of approximately 0.85 nm. However, the AFM image of the 18-nm-thick $LiMn_xO_y/Alq_3$ film shows a relatively rough and uneven surface with a mean roughness of approximately 3.02 nm, which cannot add support to the observation of Zhan *et al.* The improvement indicates that some other mechanisms are operating.

Since the electrochemical properties of $LiMn_2O_4$ might be affected by surface morphologies which are dependent on preparation methods, to shed more light on understanding the mechanism (or mechanisms) of thermally deposited $LiMn_xO_y$ films resulting in improved performance and lifetime, it is important to know the nature of the interfaces, as well as the deposited $LiMn_xO_y$ chemical content. In this regard, studies using time-of-flight secondary ion mass spectroscopy, and angle-resolved high-resolution x-ray photoelectron spectroscopy, of the deposited $LiMn_xO_y$ film, as well as Al/insulator contact, are currently in progress.

The author would like to thank Shih-Feng Hsu, Chi-Hung Liao, and Chieh-Wei Chen for discussion and their valuable help in this work.

[1] C. W. Tang and S. A. Van Slyke, Appl. Phys. Lett. **51**, 913 (1987).
[2] L. S. Hung, Thin Solid Films **47**, 363 (2000).
[3] J. Kido, K. Nagai, and Y. Okamoto, IEEE Trans. Electron Devices **40**, 1342 (1993).
[4] T. Wakimoto, Y. Fukuda, K. Nagayama, A. Yokoi, H. Nakada, and M. Tsuchida, IEEE Trans. Electron Devices **44**, 1245 (1997).
[5] L. S. Hung, C. W. Tang, and M. G. Mason, Appl. Phys. Lett. **70**, 152 (1997).
[6] J. Kido and T. Matsumoto, Appl. Phys. Lett. **73**, 2866 (1998).
[7] Y. Shimakawa, T. Numata, and J. Tabuchi, J. Solid State Chem. **131**, 138 (1997).
[8] H. Kawata, M. Nagatab, H. Kageyamac, H. Tukamoto, and A. R. West, Electrochim. Acta **45**, 315 (1999).
[9] C. V. Ramana, M. Massot, and C. M. Julien, Surf. Interface Anal. **37**, 412 (2005).
[10] S. A. Van Slyke, C. H. Chen, and C. W. Tang, Appl. Phys. Lett. **69**, 2160 (1996).
[11] Y. Gao, K. T. Park, and B. R. Hsieh, J. Appl. Phys. **73**, 7894 (1993).
[12] Y. Gao, K. T. Park, and B. R. Hsieh, J. Chem. Phys. **97**, 6991 (1992).
[13] S. A. Jeglinski, O. Amir, X. Wei, Z. V. Vardeny, J. Shinar, T. Cerkvenik, W. Chen, and T. J. Barton, Appl. Phys. Lett. **67**, 3960 (1995).
[14] F. Li, H. Tang, J. Anderegg, and J. Shinar, Appl. Phys. Lett. **70**, 1233 (1997).
[15] L. S. Hung, R. Q. Zhang, P. He, and G. Mason, J. Phys. D **35**, 103 (2002).
[16] M. G. Mason, C. W. Tang, L. S. Hung, P. Raychaudhuri, J. Madathil, L. Yan, Q. T. Le, Y. Gao, S.-T. Lee, L. S. Liao, L. F. Cheng, W. R. Salaneck, D. A. dos Santos, and J. L. Brédas, J. Appl. Phys. **89**, 2756 (2001).
[17] Q. T. Le, L. Yan, Y. Gao, M. G. Mason, D. J. Giesen, and C. W. Tang, Appl. Phys. Lett. **87**, 375 (2000).
[18] E. I. Haskal, A. Curioni, P. F. Seidler, and W. Andreoni, Appl. Phys. Lett. **71**, 1151 (1997).
[19] K. L. Wang, B. Lai, M. Lu, X. Zhou, L. S. Liao, X. M. Ding, X. Y. Hou, and S. T. Lee, Thin Solid Films **363**, 178 (2000).
[20] Y. Q. Zhan, Z. H. Xiong, H. Z. Shi, S. T. Zhang, Z. Xu, G. Y. Zhong, J. He, J. M. Zhao, Z. J. Wang, E. Obbard, H. J. Ding, X. J. Wang, X. M. Ding, W. Huang, and X. Y. Hou, Appl. Phys. Lett. **83**, 1656 (2003).